ADVANCED MATERIALS

DOI: 10.1002/adma.200801764

Low-Temperature Deterministic Growth of Ge Nanowires Using Cu Solid Catalysts**

By *Kibum Kang, Dong An Kim, Hyun-Seung Lee, Cheol-Joo Kim, Jee-Eun Yang,* and *Moon-Ho Jo**

One-dimensional crystal growth essentially exploits the highly asymmetric growth kinetics in the radial and axial directions, and often effectively employs metal-nanoparticle catalysts for dimensionally confined nucleation and the subsequent one-dimensional crystal growth.[1–3] One of the earliest and prevailing examples of such one-dimensional growth is the so-called vapor-liquid-solid (VLS) syntheses of semiconductor nanowires (NWs), where one-dimensional crystals precipitate out of the supersaturated eutectic liquids formed by the catalytic decomposition of gas precursors for given reactions.[4,5] Recently it was also found that the specific phase of the catalysts is not necessarily the eutectic liquids during the reactions, but can be the solids as well. In fact, synthetic routes from the solid-catalysts, often referred as the vapor-solid-solid (VSS) growth, are evident by the accumulating examples of semiconductor-catalyst systems, such as Si-Ti,[6] Ge-Ni,[7] GaAs-Au,[8] InAs-Au,[9] Si-Al,[10] Si-Cu,[11] Mn-Ge[12] and Ge-Au[13]. Therein it has been commonly documented that NW crystallization can be available by solid-phase diffusion of semiconductor elements through the solid catalysts.[8] One of the urgent technological breakthrough for the practical applications of the bottom-up semiconductor NWs is integrated NW array growth in large-areas with massive parallelism, and this can be achievable by deterministic growth from the ordered catalyst arrays with one-to-one relation in size and position between catalysts and nanowires.[14] In this prospect, VSS growth can potentially provide advantages for ordered array growth, by which the position and the size of individual NWs can be more predictably determined, since the surface migration and coalescence of the solid catalysts can be effectively suppressed during the growth reactions, as opposed to the case of the liquid catalysts.[15,16] Here by using Cu-catalysts, we report the low-temperature growth of Ge NWs at as low as 200 °C in a deterministic manner, so that the diameter of Ge NWs is uniformly distributed at 7 nm, directly templated from the identical size of Cu catalysts, with consistent [011] crystallographic orientation. Specifically it was found that the Cu catalyst tips are consistently orthorhombic Cu_3Ge with the heteroepitaxial relation with the cubic Ge NWs, as $[010]_{tip}//[011]_{NW,}$ along the wire axes. We attribute the low-temperature growth of 200 °C, which is well below the Cu-Ge eutectic temperature of 644 °C, to the growth by the catalytic decomposition of Ge precursors onto the *solid-phase* Cu catalysts, and describe distinct manifestations of the solid-catalytic growth from the parallel comparison to the growth from the eutectic liquids catalysts. We further demonstrate that the solid-catalytic growth in our study can be readily adapted for vertical growth by an epitaxial manner on Si substrates. We argue that the low-temperature growth of semiconductor NWs using the solid catalysts can be generally accessible, provided that the appropriate combination of solid catalysts and semiconductors are thermodynamically available, thus suggest implication for the potential large-area integrated growth on various substrates.

Figure 1a is the equilibrium Ge-Cu binary phase diagram,[17] where the Cu content is relevant to our growth temperatures. We first note that the Ge-Cu eutectic temperature of 644 °C is rather too high to expect to grow Ge NWs by the conventional VLS mechanism, because in this temperature range the thermal decomposition of GeH_4 becomes homogeneously active over the catalytic decomposition.[18,19] Instead we have observed very reproducible Ge NW growth in the temperature range of 200–275 °C, which is well below the eutectic temperature by 370–450 °C. Figure 1b shows a representative scanning electron microscopy (SEM) image of such NWs grown at 275 °C on 300 nm thick SiO_2/Si (100) substrates under 150 Torr of GeH_4, and the X-ray diffraction peaks in the inset accordingly correspond to (111), (220) and (311) of the diamond structure of Ge. We found that Ge NWs are tapered above 275 °C, and the growth is persistent down to 200 °C, as evident in the upper inset of Figure 1c. The low temperature CVD growth in this temperature range can be readily adapted to the growth on flexible polymeric substrates such as polyimide and polyarylate substrates at 260 °C, as shown in Figure 1c. The transmission electron microscope (TEM) images and energy dispersive X-ray spectra of individual NWs in Figure 2 show that the NW stems are pure Ge without the trace of Cu within the instrumental limit, whereas the tip is abundant with Cu. High resolution images in Figure 2b and c,

[*] Prof. M.-H. Jo, K. Kang, D. A. Kim, H.-S. Lee, C.-J. Kim, J.-Y. Yang
Department of Materials Science and Engineering
Pohang University of Science and Technology (POSTECH)
San 31, Hyoja-Dong, Nam Gu, Pohang, Gyungbuk 790-784 (Korea)
E-mail: mhjo@postech.ac.kr

[**] The authors thank Profs. Hyungjun Kim and Byeong-Joo Lee for helpful discussions. This research was supported by Nano R&D program through the KOSEF (2007-02864), the "System IC 2010" program by the MOCIE, the MOST-AFOSR NBIT 2007 Program funded through the KICOS (No. K20716000006-07A0400-00610), the Korean Research Foundation Grant from MOEHRD (KRF-2005-005-J13103), and Samsung Electronics. Supporting Information is available online from Wiley InterScience or from the author.

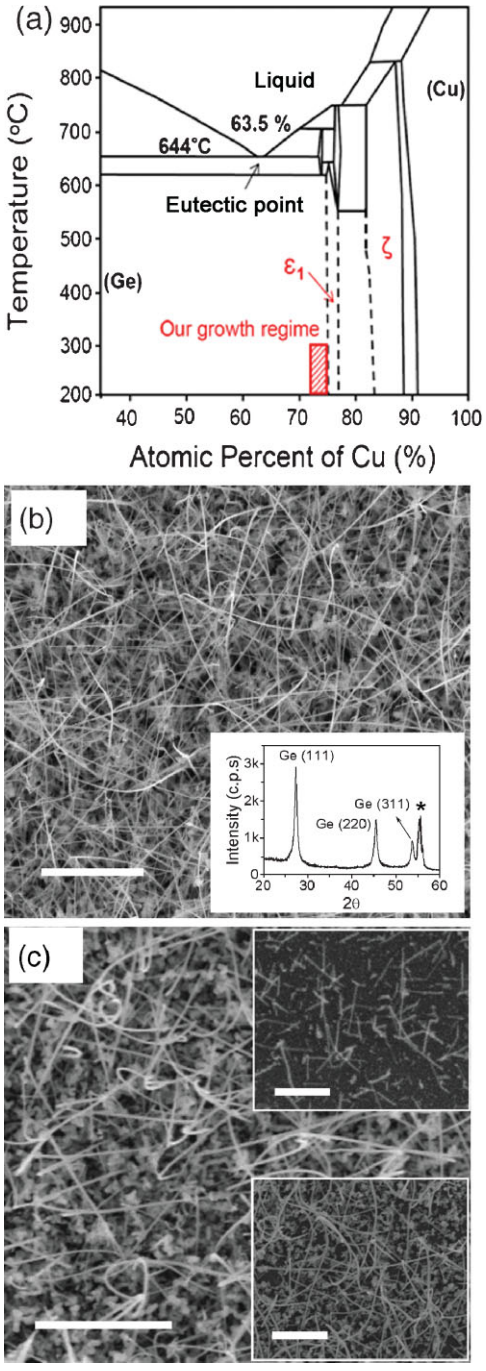

Figure 1. a) A part of the equilibrium Cu-Ge binary alloy phase diagram, relevant to our growth. b) A plan-view scanning electron microscope (SEM) image of Ge nanowires grown at 275 °C. The scale bar is 1 μm. The inset shows a representative X-ray diffraction pattern from the Ge nanowires on SiO_2/Si substrate. The star mark indicates the peak from the Si substrate. c) A representative plan-view SEM images of Ge nanowires grown on polyimide and polyarylate (the lower inset) at 260 °C. The scale bar is 1 μm. The upper inset is a SEM image of Ge nanowires grown at 200 °C. The scale bar is 200 nm.

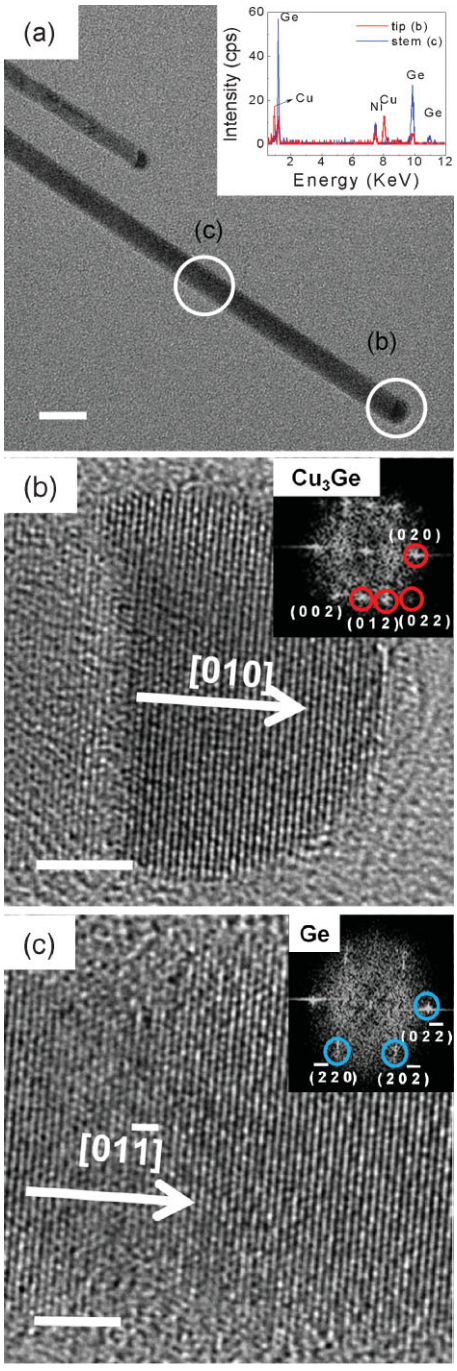

Figure 2. a) A TEM image of an individual Ge nanowire, showing the tip at the end with a dark contrast. The scale bar is 10 nm. The inset shows energy dispersive X-ray spectra collected from the tip and the stem of the nanowires, marked with circles in (a). b) A high-resolution TEM image and the corresponding fast Fourier transformation diffraction pattern (FFT-DP) indexed to Cu_3Ge at the tip region, indicating the crystal orientation along the length is [010]. The scale bar is 2 nm. c) A high-resolution TEM image and the corresponding FFT-DP indexed to Ge at the stem region, indicating the crystal orientation along the length is [01$\bar{1}$]. The scale bar is 2 nm.

ADVANCED MATERIALS

demonstrate that both the tip and the stem are single-crystalline, and are respectively indexed to orthorhombic Cu_3Ge and cubic Ge by the fast Fourier transformation diffraction patterns, as in the insets. We have examined more than five sets of NWs from different sample batches grown at the temperature range of 200–330 °C, and consistently found that the crystal phases of the tip and the stem are Cu_3Ge and Ge — see also Supporting Information. It was also found that the crystal orientations of the tip and the stem are consistently ⟨010⟩ and ⟨011⟩ in their symmetries along the wire axes, thereby the heteroepitaxial relation with cubic Ge NWs is established as $[010]_{tip}//[011]_{NW}$. The crystal orientations of semiconductor NWs by the VLS are known to be strongly dependent on their diameters, and our observation that the NWs with sub-10-nm diameter grow preferentially along [110] is consistent with literature.[20,21] Interestingly the shapes of the Cu_3Ge tips are not always hemispheric, as typically observed from Au-catalytically grown Ge NWs, and they are sometime elongated along the wire axes with rather irregular interfaces with Ge NWs,[7] as seen in Figure 3a and b.

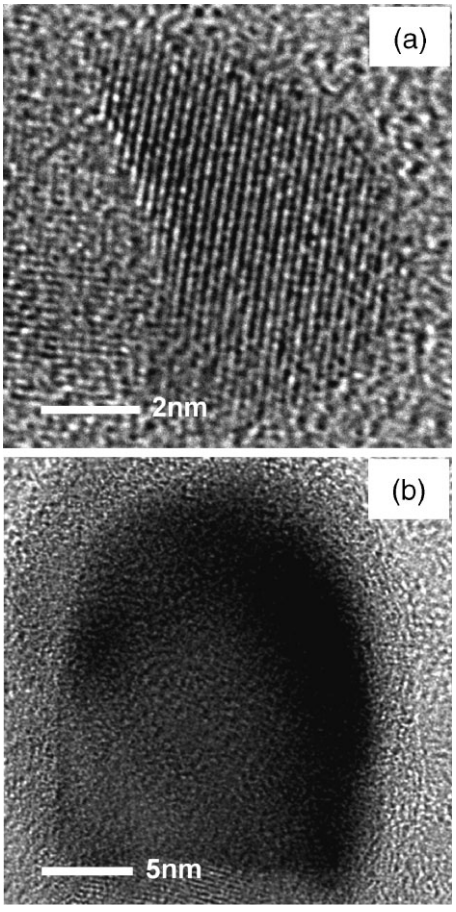

Figure 3. a, b) Transmission electron microscope images of an individual Ge nanowire at the tip regions from various samples, showing rather non-hemespheric shapes and irregular interfaces between the tip and the stem.

The coherent ⟨011⟩ crystal orientation of Ge NWs can be adapted for the vertical array growth on (011) Si substrates, provided that the heteroepitaxial growth is available between Ge NWs and Si substrates via Cu catalysts. Indeed the high resolution TEM (HRTEM) images near the interface between Ge NWs and Si substrates in Fig. 4 demonstrate the growth is

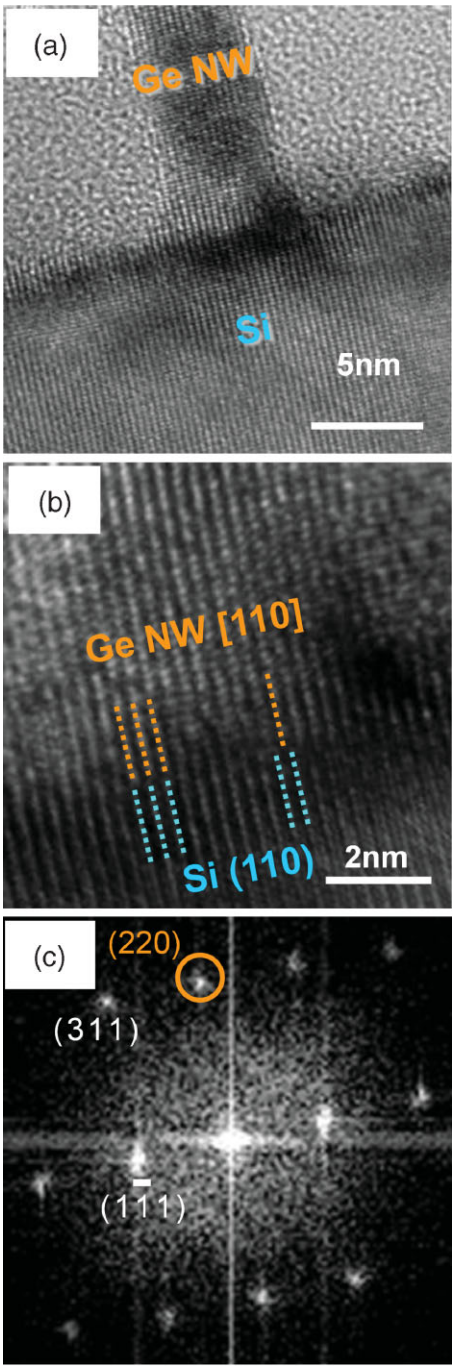

Figure 4. a) HRTEM image of a vertically grown Ge NW on Si (110) substrate. b) Interfacial HRTEM image between a Ge NW and a Si substrate. The lines parallel to the Ge ⟨110⟩ (orange) are matched to the lines normal to the Si (110) planes (blue) with the presence of misfit dislocations. c) Fast Fourier transformation diffraction patterns from (b).

established in such a heteroepitaxial manner. A closer observation at the interfaces of in Figure 4b, together with its corresponding Fourier transformation diffraction patterns in Fig. 4c, further verifies that Ge NWs grows heteroepitaxially along the [110] direction on (110) Si substrates. The lines parallel to the Ge ⟨110⟩ (orange) in Figure 4b are matched to the lines normal to the Si (110) planes (blue) with the presence of misfit dislocations presumably due to the lattice mismatch between Si and Ge. Such epitaxial growth is further extended for the Ge ⟨110⟩ NWs growth on substrates of various crystal orientations of (111), (110) and (100), and the corresponding cross-sectional and plane view images (tilted for clarity) are presented in Figure 5. The insets of Figure 5a–f summarize the directions of Ge NWs with respect to the substrate planes, and the respective occurrence yields of the directions of NWs are presented by statistically counting NWs from the plane view images in large areas. Notably the directions of NWs are concentrated into certain directions by 94.6%, 99.9% and 91.7% on (111), (110), and (100), respectively, and they can be assigned to the directions that can be predicted from the heteroepitaxial relations between Si substrates and Ge ⟨110⟩ NWs. This finding of the high yield of directional growth by epitaxy, in turn, suggests that the crystallographic orientation of Ge NWs is mainly ⟨110⟩ along the wire axes. Particularly we comment on Figure 5c that the vertically epitaxial growth of ⟨110⟩ Ge NWs on Si (110) can be feasible, provided that the other equivalent ⟨110⟩ growth directions can be effectively suppressed; *e.g.* by the geometrical confinements of Cu-catalysts in the etchpits in Si substrates.

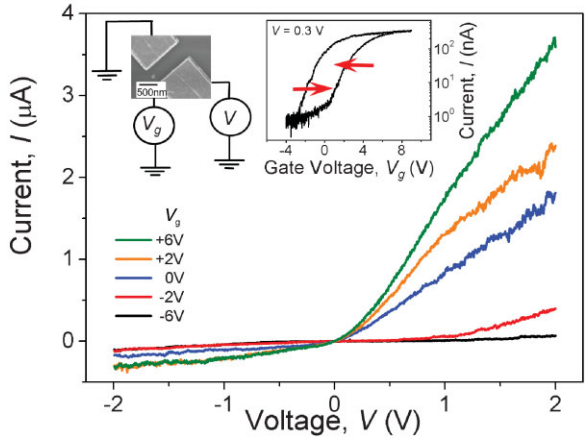

Figure 6. *I-V* characteristics recorded on a field-effect transistor (FET) incorporating an individual p-doped Ge nanowire at various gate voltages (V_g). The upper left inset is a SEM image of the representative nanowire FET along with a simplified measurement scheme. The upper middle insets are I-V_g at $V = 0.3$ V. The arrows represent the sweep direction of gate voltage.

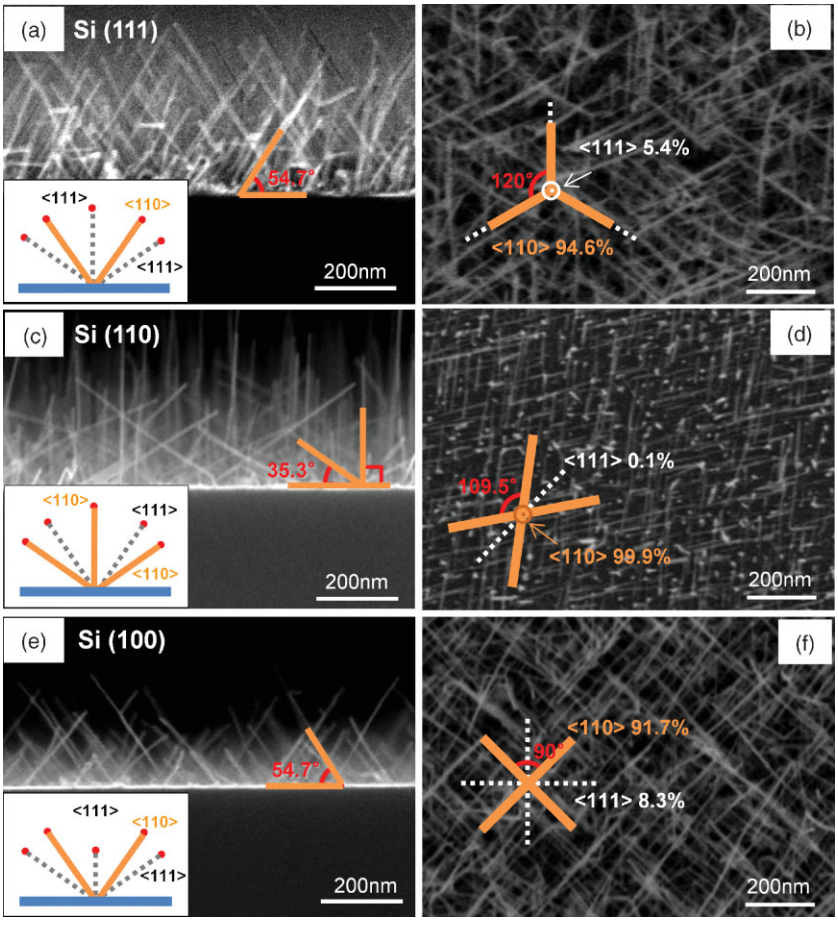

Figure 5. Series of cross-sectional and plan-view SEM images of the heteroepitaxially grown Ge NWs at 275 °C for 4.5 min on a–b) Si(111), c–d) Si(110), and e–f) Si(100) substrates, respectively. The insets in (a–f) summarize the directions of Ge NWs with respect to the substrate planes, and the respective occurrence yields of the directions of NWs.

In order to verify the basic semiconducting properties of our Ge NWs, we have fabricated a field-effect transistor (FET) incorporating individual P-doped Ge NWs on SiO_2/degenerated Si substrates, as shown in the upper left inset of Figure 6. We found that Ge NWs with B_2H_6 dopants are tapered in the same growth conditions, as also observed in the cases by the Au-catalytic growth. The main panel of Fig. 6 shows the gate voltage (V_g) dependent current (I) versus bias voltage (V), from which the resistivity is calculated to be 4.42×10^{-3} cm at $V_g = 0$V. The current was suppressed with negatively increasing of V_g, and this typical n-type FETs behavior is also shown in the I-V_g at a constant V of 0.3 V, as in the upper middle inset. We note that the current varies hysteretically to the directions of V_g sweeps, presumably due to trap charges existing at the NW/SiO_2 interface and in the oxide.[22]

Our observations that Ge NW growth is possible even at 200 °C and that the crystal structures of the catalyst tip are reproducibly

ADVANCED MATERIALS

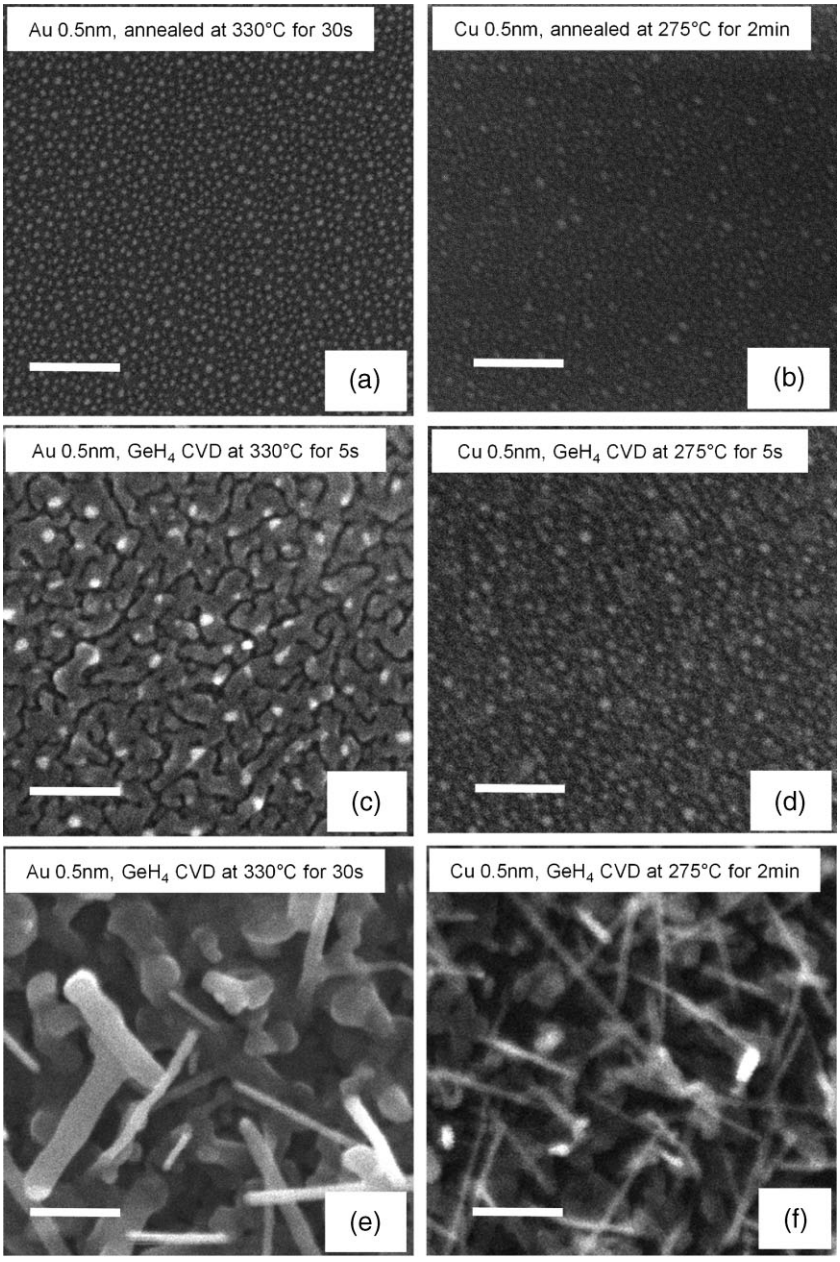

Figure 7. Sequential snap shots of the early growth stage of two different Ge nanowires grown by Au and Cu catalysts at 330 °C and 275 °C. a) 0.5-nm-thick Au films annealed at 330 °C before the growth with GeH_4, b) 0.5-nm-thick Cu films annealed at 275 °C before the growth with GeH_4, c) the initial stage of deposition with GeH_4 for 5 s on 0.5 nm thick Au films, d) the initial stage of deposition with GeH_4 for 5 s on 0.5 nm thick Cu films, e) the 30 s deposition of GeH_4 on 0.5 nm thick Au films, and f) the 2 min deposition of GeH_4 on 0.5 nm thick Cu films. All the scale bars are 100 nm.

identified as Cu_3Ge strongly suggest that the Ge crystals precipitates out from solid Cu_3Ge catalysts, e.g. by the VSS mechanism. According to the Ge-Cu phase diagram in Figure 1a between 200–330 °C, the Ge-Cu systems involves several intermediate phases of solid-solutions such as ε_1 and ς with the Cu content ranged as 74.9–76.9% and 81.7–88.5%, respectively. Alternatively the ε_1 and ς phases are often denoted as Cu_3Ge and Cu_5Ge; for example, ε_1 phase is referred as Cu_3Ge solid-solution, where the Cu content varies around the mean content of 75% by −0.1–+1.9%. We then speculate that the Ge precipitates out from the super-saturated Cu_3Ge with Cu by up to 1.9% to form Ge NWs, provided that an efficient diffusion across the catalysts is established during the reactions. A qualitatively similar VSS growth of Si NWs was reported using Al catalysts at the temperature as low as 430 °C, where the Si solubility in Al is approximately less than 1%.[10] Therein the solubility of Si in Al is negligible below 400 °C, and this limited solubility presumably imposes the lower limit of the growth temperature. In the Ge-Cu system, however, the Ge solubility in Cu_3Ge is persistently present down to 200 °C from the eutectic temperature, and thus Ge NW growth from the solid Cu_3Ge catalysts can be achievable at such low temperatures. This finding raises an interesting point that upon the existence of thermodynamically available solid-catalysts the appropriate solubility of semiconductors in such solid-catalysts can be an important indicator to determine the lower limit of the attainable growth temperatures.

In order to further observe manifestations of the VSS growth in our study, we performed a series of control growth of Ge NWs using Au catalysts prepared by the same way as Cu catalysts, for parallel comparison to the VLS growth. Fig. 7 shows the sequential snap shots of the early growth stages of two different Ge NWs grown by Au and Cu catalysts at 330 °C and 275 °C in parallel, so that they would represent the VLS and VSS growth. The comparison clearly illustrates and contrasts how the Ge NW growth evolves from two different types of catalysts. The Au catalysts were initially scattered as individual nanosized grains, as in Figure 7a, and then coalesced into larger grains with embryonic NWs in the very early stage of 5 s growth shown in Figure 7c, which suggest that the catalysts are in liquid phases. In the later stage of 30 s growth, as in Figure 7e, the diameters of the constituent NWs diverge in their distribution. Meanwhile the Cu catalysts remain as individual grains with mean diameter of 7.1 nm without any obvious grain growth at the growth temperature, and lead to growth with uniform diameters, as consecutively seen in Figure 7b, d and f. Figure 8a shows the statistical diameter distribution of as-prepared Cu catalysts and the resultant Ge NWs, examined by SEM and TEM, and they both show a very similar distribution centered at 7 nm, that is, we

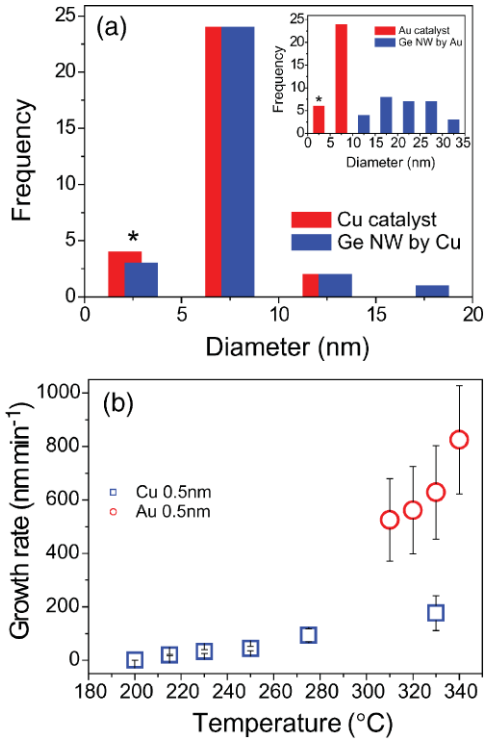

Figure 8. a) The histogram of the diameter distribution for Cu catalysts (0.5 nm thick Cu films, as shown in Fig. 7a) and the resultant Ge nanowires. The inset shows the same information for Au catalysts. Diameters were measured by SEM and TEM, and there is uncertainty at the values below 5 nm, marked with a star, due to the limited spatial resolution. b) The growth rate of Ge nanowires as a function of temperature for the Cu-catalytic growth and the Au-catalytic growth at different temperature regimes.

find the diameters of Ge NWs are directly templated from those of Cu catalysts with the one-to-one deterministic manner in their diameters, whereas in the case of Au-catalytic Ge NWs, as shown in the inset, the diameter of Ge NWs is ranged in a rather wider distribution, displaying the mean NW diameter of 20 nm from the mean catalyst diameter of 6.5 nm. The observation of the uniform diameter distribution of Ge NWs directly templated from that of Cu-catalysts suggests that the Cu_3Ge catalysts are in solid phases, and the detrimental coalescence of catalysts that is often observed with liquid catalysts can be effectively suppressed during the growth reactions. This finding provides practical implication that the NW diameter distribution can be deterministically controllable for large-area integrations of NWs with massive parallelism, when NWs grow by solid-catalysts. We also comment here that in the solid-catalytic NW growth the one-to-one deterministic definition of positions between catalysts and NWs can be also feasible, provided the surface diffusion of catalysts is effectively suppressed. We are under further investigation on this aspect. We note that Cu-catalytic growth of Si NWs at 500–650 °C was also reported; thereby the growth is similarly interpreted as the VSS mechanism.[11] However they lack in the coherent size relations between catalysts and NWs, presumably due to the relatively high growth temperatures. The VSS NW growth can be also manifested in the growth kinetics, compared to the VLS, and we found that the growth rate (in the unit of nm min^{-1}) for the Cu-catalyzed NWs is strongly suppressed by almost an order of magnitude, as shown in Figure 7b. It is presumably due to a weaker desorption of GeH_4 and/or a lower diffusivity of Ge in the solid-Cu_3Ge catalytic growth than in the liquid-Au catalytic growth.

In summary, we report an unprecedentedly low temperature synthetic route of uniformly sub-10-nm thick Ge NWs employing Cu catalysts, which is readily adapted to the growth on flexible polymer substrates. We showed that the catalyst tips are consistently orthorhombic Cu_3Ge with their heteroepitaxial relation with the cubic Ge NWs, as $[010]_{tip}//[011]_{NW}$, and attribute the attainable low temperature growth with the uniform diameter distribution to the fact that the Ge NW growth occurs from solid-phase Cu_3Ge catalysts, e.g. by the VSS. Specifically, the VSS NW growth from Cu catalysts in our study is manifested, in contrasts to the VLS growth by Au catalysts, as i) the low temperature growth at as low as 200 °C with ii) the uniform NW diameter control. We argue that our principal observations suggest important implication for the potential large-area integrated growth of semiconductor NWs.

Experimental

Synthesis: Our NW syntheses began with the preparation of Cu-catalysts by deposition of discontinuous Cu films of the nominal thickness of 0.5 nm on various substrates including SiO_2/Si (100) and flexible polymer substrates such as polyimide and polyarylate. We note that Cu colloidal nanoparticles are not commercially available and thus are not considered for catalysts in our syntheses. The Cu-coated substrates were subsequently loaded into a hot-walled quartz-tube furnace, where we carried out chemical vapor deposition (CVD) of GeH_4 as a Ge precursor (specifically, 10% of GeH_4 diluted in high purity H_2) at given temperatures (200–330 °C) and gas pressures (30–150 Torr).

Charaterization: The Ge nanowires were characterized by scanning electron microscopy (SEM) for their morphology, and by transmission electron microscopy (TEM) and energy dispersive X-ray spectroscopy (EDX) for their crystallinity and composition.

Device fablication: We fabricated a field-effect transistor (FET) incorporating individual p-doped Ge NWs on SiO_2/degenerated Si substrates by e-beam lithography and Ti/Au (15/100 nm) lift-off. p-doped Ge NWs without tapering were grown with PH_3 (100 ppm diluted in H_2) at the relative pressure ratio of GeH_4: PH_3 of 1: 6.7×10^{-5}.

Received: June 24, 2008
Revised: August 11, 2008
Published online: October 15, 2008

[1] L. Manna, D. J. Milliron, A. Meisel, E. C. Scher, A. P. Alivisatos, *Nat. Mater.* **2003**, *2*, 382.
[2] Y. Xia, P. Yang, Y. Sun, Y. Wu, B. Mayers, B. Gates, Y. Yin, F. Kim, H. Yan, *Adv. Mater.* **2003**, *15*, 353.
[3] A recent review: C. M. Lieber, Z. L. Wang, *MRS Bull.* **2007**, *32*, 99.
[4] R. S. Wagner, W. C. Eliis, *Appl. Phys. Lett.* **1964**, *4*, 89.

ADVANCED MATERIALS

[5] A. M. Morales, C. M. Lieber, *Science* **1998**, *279*, 208.
[6] T. I. Kamins, S. R. Williams, D. P. Basile, T. Hesjedal, J. S. Harris, *J. Appl. Phys.* **2001**, *89*, 1008.
[7] a) H.-Y. Tuan, D. C. Lee, T. Hanrath, B. A. Korgel, *Chem. Mater.* **2005**, *17*, 5705. b) S. Hofmann, Ch. Sharma, R. Wirth, F. Cervantes-Sod, C. Ducati, T. Kasama, R. E. Dunin-Borokowski, J. Druckers, P. Bennett, J. Robertson, *Nat. Mater.* **2008**, *7*, 372.
[8] A. I. Persson, M. W. Larsson, S. Stenström, B. J. Ohlsson, L. Samuelson, L. R. Wallenberg, *Nat. Mater.* **2004**, *3*, 677.
[9] K. A. Dick, K. Deppert, T. Mårtensson, B. Mandl, L. Samuelson, W. Seifert, *Nano Lett.* **2005**, *5*, 761.
[10] Y. Wang, V. Schmidt, S. Senz, U. Gösele, *Nat. Nanotechnol.* **2006**, *1*, 186.
[11] a) J. Arbiol, B. Kalache, P. R. I. Cabarrocas, J. R. Morante, A. F. I. Morral, *Nanotechnology* **2007**, *18*, 305606. b) Y. Yao, S. Fan, *Mater. Lett.* **2007**, *61*, 177.
[12] J. L. Lensch-Falk, E. R. Hemesath, F. J. Lopez, L. J. Laugon, *J. Am. Chem. Soc.* **2007**, *129*, 10670.
[13] S. Kodambaka, J. Tersoff, M. C. Reuter, F. M. Ross, *Science* **2007**, *316*, 729.
[14] a) D. Wang, R. Tu, L. Zhang, H. Dai, *Angew. Chem. Int. Ed.* **2005**, *44*, 2. b) Y. Yao, S. Fan, *Mater. Lett.* **2007**, *61*, 177.
[15] J. B. Hannon, S. Kodambaka, F. M. Ross, R. M. Tromp, *Nature* **2006**, *440*, 69.
[16] K. Takahiro, M. Tatsunori, N. Tohru, T. Hideo, S. Tohru, K. Kazunori, F. Minoru, *Nano. Lett.* **2008**, *8*, 362.
[17] *Binary Alloy Phase Diagram*, Vol. 1, 2nd ed., ASM International, Materials Park, OH **1990**.
[18] C.-B. Jin, J.-E. Yang, M.-H. Jo, *Appl. Phys. Lett.* **2006**, *88*, 193105.
[19] J.-E. Yang, C.-B. Jin, C.-J. Kim, M.-H. Jo, *Nano. Lett.* **2006**, *6*, 2679.
[20] Y. Wu, Y. Cui, L. Huynh, C. J. Barrelet, D. C. Bell, C. M. Lieber, *Nano Lett.* **2004**, *4*, 433.
[21] V. Schmidt, S. Senz, U. Gösele, *Nano Lett.* **2005**, *5*, 931.
[22] C.-J. Kim, W.-H. Park, J.-E. Yang, H.-S. Lee, S. Maeng, Z. H. Kim, M.-H. Jo, *Appl. Phys. Lett.* **2007**, *91*, 033104.